Solid State Communications 250 (2017) 57–63

Contents lists available at ScienceDirect

Solid State Communications

journal homepage: www.elsevier.com/locate/ssc

Communication

Magnetic field effects on the DOS of a Kondo quantum dot coupled to LL leads

Kai-Hua Yang[a,*], Chang-Dong Qin[a], Huai-Yu Wang[b], Xu Wang[a]

[a] College of Applied Sciences, Beijing University of Technology, Beijing 100122, China
[b] Department of Physics, Tsinghua University, Beijing 100084, China

ARTICLE INFO

Keywords:
Luttinger liquid
Kondo regime
Density of states
Quantum dot
Magnetic field

ABSTRACT

We investigate the joint effects of a magnetic field and electron-electron interaction on the tunneling density of states (DOS) of a quantum dot coupled to the Luttinger liquid leads in the Kondo regime. We find that for intralead electron interaction, the DOS develops two peaks deviated from the origin by the Zeeman energy. With the increase of the intralead interaction, a phase transition occurs. For moderately strong interaction, the Zeeman splitting peaks develop into two dips. The splitting of the Kondo peak and dip is not symmetric with respect to up and down spins. In the limit of strong interaction the Zeeman splitting behavior disappears and there appears a power-law scaling behavior.

1. Introduction

With techniques in manufacturing devices of nanometer scale, research on thelow-dimensional electronic systems has become a very active field in condensed matter physics. Low-dimensional systems may exhibit intricate strongly correlated phenomena, such as the Kondo effect [1] and Luttinger liquid (LL) paradigm [2]. The Kondo effect was first discovered in metals with magnetic impurities and was caused by the many-body screening of an impurity spin by itinerant electrons. It lead to appearance of a narrow low-energy resonance in the impurity density of state(DOS) at low temperature [1]. The Kondo effect was also observed in quantum dot (QD) systems [3–5]. This reflected an interesting many-body phenomenon in the nanophysics field and has attracted an increased experimental and theoretical enthusiasm. To probe the spin physics clearly, it is inevitable to study the effect of a magnetic field on the properties of the electron systems. In probing the formation of Kondo resonances and the influence of the spin-dependent renormalization of the dot level on spin fluctuations, magnetic field is a particularly important tool. There have appeared many experimental [3,6–10] and theoretical [11–18] study of the effects of magnetic field in QD systems. These works revealed that the Kondo anomaly would split and be suppressed by an external magnetic field. In these works, the leads were traditional ones, i.e., they were taken to be Fermi liquids (FLs) and interactions in the leads were ignored. This is sufficient if the leads are two or three dimensional electron gases, where interactions affect the low energy properties only perturbatively. However, in one dimension, arbitrarily weak interactions completely modify the ground state, and the low energy excitations are governed not by FL theory but instead by the LL [2]. In contrast to a LL, the low energy excitations in a LL are spin and charge density fluctuations, and there are no well-defined single particle excitations. Moreover, the speeds of the spin and charge density fluctuations are different, i.e., spin and charge separate [19]. Naturally, one may ask whether the magnetic field effect on the DOS is different from that of FLs, say the Zeeman splitting. To our knowledge, the theoretical research of the effect of a magnetic field on a QD system with LL leads has not been seen yet.

In the present work, we study the tunneling DOSs of the QD weakly coupled to LL leads, with the extended equation-of-motion (EOM) method of the nonequilibrium Green functions. This approach has the advantage of intuitiveness and can provide a semi-quantitative understanding of the Kondo effect in this case. For weak intralead interaction, the Kondo peak splits into two located at energies $\omega = \pm g\mu_B B$, where $g\mu_B B$ is the Zeeman energy. The peak heights are proportional to the electron-electron interaction constant, which is not accessible in a measurement of the conventional zero bias anoumaly (ZBA).

When the intralead interaction become moderately strong, the Kondo peaks develop into dips with no shift of the location. This manifests that single-electron picture is valid for a weak electron-electron interaction only, and is not applicable to the case of a strong repulsion between electrons. In fact in carbon nanotubes, the interaction in the lead is strong, and an electron-like quasiparticle is not valid. With the further increase of the intralead interaction, the DOS features power-law behavior near the Fermi energy. The exponent in this power

* Corresponding author.
E-mail address: khy@bjut.edu.cn (K.-H. Yang).

http://dx.doi.org/10.1016/j.ssc.2016.11.017
Received 18 February 2016; Received in revised form 2 September 2016; Accepted 18 November 2016
Available online 20 November 2016
0038-1098/

law is actually determined by LL physics alone.

The paper is organized as follows. In Section 2 we present our model of a strongly correlated QD in the presence of a magnetic field. The expressions for numerically evaluating the QD DOS resulting from an effective Keldysh field theory are given. In Section 3 the discussions of our numerical results are given and finally we summarize our findings in Section 4.

2. Theoretical model and method

The system is modeled by the Hamiltonian:

$$H = H_{L/R} + H_D(t) + H_T, \tag{1}$$

where the H_D and $H_{L/R}$ describe the uncoupled QD and semi-infinite left/right LL leads, respectively. H_T is the tunneling Hamiltonian between the QD and the leads. In the bosonized form $H_{L/R}$ can be written as [20–22]:

$$H_\alpha = \hbar \int_0^\infty k\,(v_{\alpha c} a_{k\alpha}^\dagger a_{k\alpha} + v_{\alpha s} c_{k\alpha}^\dagger c_{k\alpha}) dk,\ (\alpha = L, R), \tag{2}$$

Where the operator $a_{k,\alpha}$ and $c_{k,\alpha}$ in lead α=L or Rare the annihilation operator of bosons describing charge and spin density fluctuations propagating with velocity $v_{\alpha c}$ and $v_{\alpha s}$, respectively. The Hamiltonian of the dot with an on-site Coulomb repulsion U is

$$H_D = \sum_\sigma (\varepsilon_{d\sigma} + \sigma g\mu_B B) d_\sigma^\dagger d_\sigma + U d_\uparrow^\dagger d_\uparrow d_\downarrow^\dagger d_\downarrow. \tag{3}$$

Here $d_\sigma^\dagger$ and d_σ are the creation and annihilation operators of electrons with spin-σ (σ=↑,↓) on the QD, $\varepsilon_{d\sigma}$ is the energy level of the dot in the absence of the external magnetic field B, g is the Landé factor and μ_B is the Bohr magneton. The second term in Eq. (3) describes the Coulomb interaction U. In the following we take the limit $U \to \infty$, which forbids the double occupancy of the dot level. The last term in Eq. (1)H_T describes the coupling between the QD and interacting LL leads.

$$H_T = \sum_{\alpha\sigma} (t_\alpha d^\dagger \psi_{\alpha,\sigma} + h.\,c.\,) \tag{4}$$

in which t_α stands for the tunneling amplitudes between the QD and conduction lead α.$\psi_{\alpha\sigma}^\dagger$and $\psi_{\alpha\sigma}$are the Fermi operators at the end points of the α lead, which can be written in a bosonized form [20,21]:

$$\psi_{\alpha\sigma} = \sqrt{\frac{2}{\pi\alpha'}} \exp[\int_0^\infty dk e^{-\alpha' k/2} (\frac{a_{k\alpha} - a_{k\alpha}^+}{\sqrt{2K_{\alpha c} k}} + \sigma \frac{c_{k\alpha} - c_{k\alpha}^\dagger}{\sqrt{2kK_{\alpha s}}})], \tag{5}$$

where α' is a short-distance cut-off with the same order of magnitude of the reciprocal of the Fermi wave numberk_F. The intra-lead electron interaction parameter for the α lead is $K_{\alpha c}$ for the charge sector and $K_{\alpha s}$ for the spin sector. It is well known that $K_{\alpha s}$=1, and we simply denote $K_{\alpha c}$=K_α. In this paper, we use natural units such that e=$\hbar$=k_B=1.

In the following, we derive the formulas for the spin resolved spectral density:$\rho_\sigma(\omega) = -\frac{1}{\pi}\mathrm{Im}G_\sigma^r(\omega)$.$G_\sigma^r(\omega)$denotes the Fourier transformation of the retarded Green function of the on-dot electron $G_{d\sigma}^r(t-t') = -i\theta(t)\langle\{d_\sigma^\dagger(t'), d_\sigma(t)\}\rangle$. In order to calculate the $G_\sigma^r(\omega)$, we use the EOM method. In the first step, we follow the standard procedure to take the derivative of $G_{d\sigma}^r(t-t')$with respect to time t:

$$(i\frac{\partial}{\partial t} - \varepsilon_{d\sigma}) G_{d\sigma}^r(t,t') = \delta(t-t') + U\langle\langle d_\sigma(t) n_{\bar\sigma}(t); d_\sigma^\dagger(t')\rangle\rangle^r + \sum_\alpha t_\alpha \langle\langle \psi_{\alpha\sigma}(t); d_\sigma^\dagger(t')\rangle\rangle^r, \tag{6}$$

where $\langle\langle O_1(t); O_2^\dagger(t')\rangle\rangle = -i\theta(t-t')\langle\{O_1(t), O_2^\dagger(t')\}\rangle$. Here the curl brackets mean the anti-commutator of the operators. On the right hand side of Eq. (6), the second higher order Green's functions $\langle\langle d_\sigma(t) n_{\bar\sigma}(t); d_\sigma^\dagger(t')\rangle\rangle^rand\langle\langle \psi_{\alpha\sigma}(t); d_\sigma^\dagger(t')\rangle\rangle^r$appear. So, in the next step, we need to compute these higher order Green functions. Their EOM are written as

$$i\frac{\partial}{\partial t}\langle\langle \psi_{\alpha\sigma}(t); d_\sigma^\dagger(t')\rangle\rangle^r = t_\alpha^* G_{d\sigma}^r(t,t') + \langle\langle [\psi_{\alpha\sigma}(t), H_\alpha]; d_\sigma^\dagger(t')\rangle\rangle \tag{7}$$

and

$$(i\frac{\partial}{\partial t} - U - \varepsilon_\sigma)\langle\langle d_\sigma(t) n_{\bar\sigma}(t); d_\sigma^\dagger(t')\rangle\rangle^r = \delta(t-t') + i\sum_\alpha \{t_\alpha(t)\Gamma_{1\alpha}^{(2)}(t,t') + t_\alpha^*(t)\Gamma_{2\alpha}^{(2)}(t,t') - t_\alpha(t)\Gamma_{3\alpha}^{(2)}(t,t')\}. \tag{8}$$

For simplicity we introduce denotations for the correlations in the right of Eq. (8): $\Gamma_{1\alpha}^{(2)}(t,t')$=−i$\langle T\{\psi_{\alpha\sigma}(t) n_{\bar\sigma}(t); d_\sigma^\dagger(t')\}\rangle$, $\Gamma_{2\alpha}^{(2)}(t,t')$=−i$\langle T\{\psi_{\alpha\sigma}^\dagger(t) d_\sigma(t) d_{\bar\sigma}(t); d_\sigma^\dagger(t')\}\rangle$ and $\Gamma_{3\alpha}^{(2)(t,t')}$=$d_\sigma^\dagger(t')\}\rangle$. The EOM's of $\Gamma_{1\alpha}^{(2)}(t,t')$, $\Gamma_{2\alpha}^{(2)}(t,t')$and $\Gamma_{3\alpha}^{(2)}(t,t')$involve the third higher order Green's functions. The treatment of the third order functions are presented in Appendix A.

After the lengthy derivation, the retarded Green's function of the QD$G_{d\sigma}^r(\omega)$in the strong correlation limit $U\to\infty$ reads

$$G_{d\sigma}^r = \frac{1 - \langle n_{\bar\sigma}\rangle}{\omega - \varepsilon_{d\sigma} - \Sigma_{0,\sigma}^r - \Sigma_{1,\sigma}^r}, \tag{9}$$

where

$$\Sigma_0^r(\omega) = \sum_\alpha g_\alpha^r(\omega), \tag{10a}$$

$$g_\alpha^r(\omega) = \int \frac{d\omega'}{2\pi} \frac{A_\alpha(\omega')}{\omega - \omega'} - \frac{i}{2}\pi A_\alpha(\omega) \tag{10b}$$

and

$$\Sigma_{1,\sigma}^r(\omega) = \sum_\alpha \frac{1}{1 - (\varepsilon_{d\sigma} - \varepsilon_{d\bar\sigma}) g_\alpha^r(\omega)} \left(\int \frac{d\omega'}{2\pi} \frac{F_\alpha^<(\omega') A_\alpha(\omega')}{\omega - \omega'} - \frac{i}{2} F_\alpha^<(\omega) A_\alpha(\omega) \right). \tag{10c}$$

Here we have denoted that $\varepsilon_{d\uparrow} = \varepsilon_d + g\mu_B B$, $\varepsilon_{d\downarrow} = \varepsilon_d - g\mu_B B$ and $A_\alpha(\omega) = \Gamma_\alpha[F_\alpha^>(\omega) + F_\alpha^<(\omega)]$.

The DOS of the dot electron is

$$\rho_\sigma = -\frac{1}{\pi}\mathrm{Im}G_{d\sigma}^r(\omega). \tag{11}$$

In order to determine $\langle n_{\bar\sigma}\rangle$appearing in Eq. (9), we exploit the self-consistent equation,

$$\langle n_{\bar\sigma}\rangle = \int \frac{d\omega}{2\pi i} G_{d\bar\sigma}^<(\omega). \tag{12}$$

However, to compute the Green function $G_{d\bar\sigma}^<(\omega)$in the EOM approach is rather difficult. A procedure based on an ansatz was proposed by Ng [23]. This ansatz assumed that the lesser and greater self-energy functions have the forms $\Sigma^<(\omega) = \Sigma_0^<(\omega)X(\omega)$ and $\Sigma^>(\omega) = \Sigma_0^>(\omega)X(\omega)$. Here, the function$X(\omega)$is to be determined by the condition $\Sigma^<(\omega) - \Sigma^>(\omega) = \Sigma^r(\omega) - \Sigma^a(\omega)$where$\Sigma_0^>(\omega)$denotes the self-energy function as U=0. With this ansatz, we can rewrite Eq. (12) as

$$\langle n_{\bar\sigma}\rangle = -\frac{1}{\pi}\int d\omega \frac{\Gamma_L F_L^<(\omega) + \Gamma_R F_R^<(\omega)}{\sum_\alpha A_\alpha(\omega)} \mathrm{Im}G_{d\bar\sigma}^r(\omega). \tag{13}$$

Consequently, we are able to obtain the retarded Green function $G_{d\bar\sigma}^r(\omega)$by solving numerically this equation and Eq. (9) with $\bar\sigma$in place of σ. In the above equations, $\Gamma_\alpha$is the line width function describing the effective level broadening of the dot, $F_\alpha^<(\omega)$is the occupation number of electrons and defined by

$$F_\alpha^{>,<}(\omega) = \frac{1}{2\pi} e^{\pm\frac{\omega-\mu_\alpha}{2T}} \left(\frac{\pi T}{\Lambda}\right)^{1/g-1} \frac{1}{\Gamma(1/g_\alpha)} \left| \Gamma(\frac{1}{2g_\alpha} + i\frac{\omega-\mu_\alpha}{2\pi T}) \right|^2, \quad (\alpha = L, R), \tag{14}$$

Where Λ is the high-energy cutoff or a band width [21]. The superscript signs > and < on the left hand side correspond to the signs + and − in the exponent on the right hand side, respectively. Γ(z) is the Gamma

function and

$$g_\alpha = \frac{2}{K_\alpha^{-1} + 1}. \quad (15)$$

When K=1, the non-interaction case, Eqs. (9)–(15) will go back to those of a FL-QD-FL system under a magnetic field. In this case, the LL distribution function $F_\alpha^<(\omega)$defined in Eq. (14) will degrade to the Fermi distribution function $f(\omega)$ and$F_\alpha^>(\omega)$to 1− $f(\omega)$. The case in the absence of the magnetic field has been studied previously [24].

3. Numerical results and discussions

In the present work we address the behavior of the Kondo state in the presence of the intralead interaction and an external magnetic field in both equilibrium and nonequilibrium. For simplicity, we assume the symmetric case, K_L= K_R =K, Γ_R=Γ_L and take Γ=Γ_R+Γ_L as the energy unit. The dot level ε_d =−2.0 and the Fermi energy of the leads is set to be zero, E_F=0. Temperature T=0.000001. Such parameters are appropriate for Kondo regime [25,26]. We consider the whole range of interaction of the leads from noninteracting limit (K=1) to strong interaction case K«1. In equilibrium, the chemical potentials on the left and right leads are set to be μ_R=μ_L=0. The total DOS of the on-dot electron is the summation of the two spin DOSs, $\rho(\omega) = \rho_\uparrow(\omega)+\rho_\downarrow(\omega)$.

First, we calculate the electronic DOS $\rho(\omega)$ of the dot for non-interaction FL leads, K=1. From Fig. 1one observes that when an external magnetic field is applied, the Kondo peak splits into two peaks, compared to the spin-degenerate case. The magnetic field suppresses the Kondo effect. The distance between two peaks is $2g\mu_B B$, where $g\mu_B B$ is the Zeeman energy, which was observed in nonequilibrium transport through QDs [6–8]. The magnetic field leads to some asymmetric shapes under extremely low temperature, and the asymmetric peaks are related to the electron spin singlet and hole spin singlet, respectively. So the two channels corresponding to spin-up and spin-down electrons are no longer equivalent. The spin-down peak shifts towards the low energy, and the spin-up one towards the high energy. This indicates that the dominant contribution of $\rho_\uparrow(\omega)$to the main peak comes from the coupling of the local state with the excited conduction electron states, while that of $\rho_\downarrow(\omega)$ from the coupling with the excited hole states. It is inferred that as B=0, both spin exchange processes contribute to the main Kondo peak, and when the magnetic field increases, they decay in different rates. The Zeeman effect removes the degeneracy of the spin states and weakens the Kondo effect. The amplitude of the Kondo resonance for spin-down significantly exceeds that for spin-up. With the increasing of the field, the height of the peak at −B slightly grows up and that at B is weakly reduced. The resonances at the lower energies are much stronger than those at the higher energies.

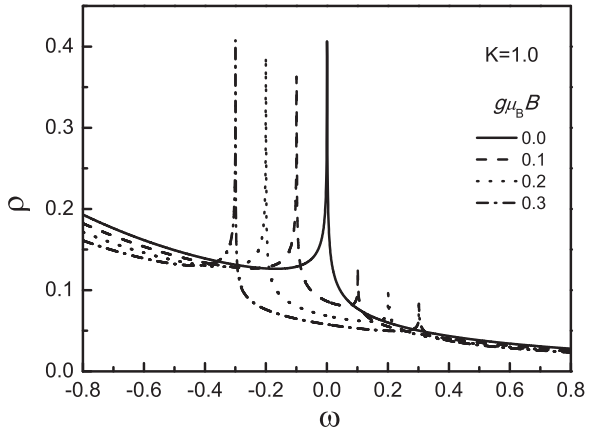

Fig. 1. The total equilibrium DOS as a function of energy ω for K=1. The figure shows the splitting of the Kondo peak for different values of the magnetic field.

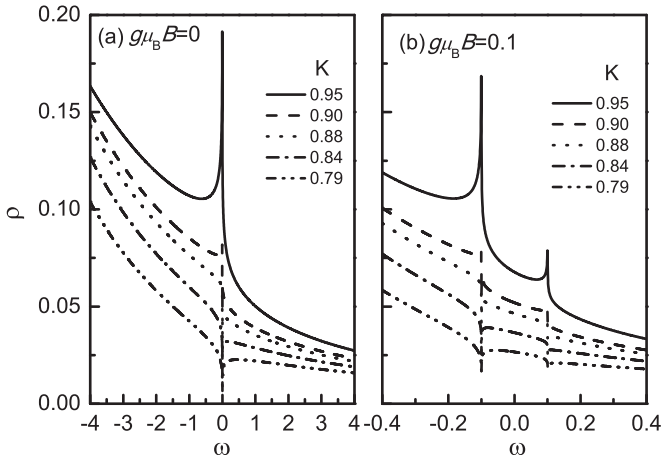

Fig. 2. The total equilibrium DOS as a function of energy ω for weak intralead interactions at a fixed magnetic field.

Now we let the intralead interaction turn on. In Fig. 2, we plot the DOS as the function of the energy ω for the weak interaction.

In Fig. 2(a), the magnetic field is absent. The DOS develops a dip at Fermi energy with the increase of the intralead interaction, which shows a stable two-channel Kondo (2CK) physics. This is caused by a local spin of the dot in the spin degenerate system antiferromagnetically coupled to two, not only one, independent electron leads. Since the electrons in the two leads do not communicate to each other, each attempts to screen the local spin, resulting in overall over screening. This exhibits fascinating low-energy LL behavior. The notion of an electron-like quasiparticle is invalid.

The introduction of a magnetic field breaks the spin degeneration. A Zeeman splitting causes the localized level of the dot to split into two, i.e., $\varepsilon_{d\uparrow}$=ε_d+$g\mu_B B$ and $\varepsilon_{d\downarrow}$=$\varepsilon_d$−$g\mu_B B$, as shown by Fig. 2(b). One can observe that the applied magnetic field splits the Kondo peak into two peaks separated by two times of $g\mu_B$B for very weak intra-lead repulsive interaction, which manifests that the single-electron picture is valid for a weak intralead electron interaction only. Compared to Fig. 1, all the peak heights decrease due to the intra-lead interaction which suppresses the electron tunneling. With the increase of the intra-lead interaction, the peaks rapidly decrease and turn into a dip-like structure which is a signature of the 2CK physics behavior. The turning point is around K=0.88. A quantum phase transition from one to 2CK physics occurs around K=0.88 into the regime where the peaks at ± $g\mu_B$B becomes two minimums. The strongest manifestation of the dip behavior can be found in carbon nanotubes, where the interaction is moderately strong.

In Fig. 3, the intralead interaction is a moderate value, K=0.74. When the magnetic field is absent, the Kondo dip located at Fermi energy indicates that the 2CK physics has already been reached because of the moderately strong interaction. A magnetic field has drastic effects on the spin resolved DOS of the dot. With the strengthening of the magnetic field, the dip depths at both ± $g\mu_B$B almost remains, a feature different from the Kondo peaks shown in Fig. 1.

In order to further show the variety of the DOS with the change of the intralead interaction K under the magnetic field, we also plot the DOS in Fig. 4 for moderately and weak intralead interactions such as K=0.7, 0.6, 0.5 and 0.4 under the fixed magnetic field. It was stressed that the dips become small with the intralead interaction strengthening.

At low energy it is well known that the spectral function as a function of energy is suppressed and behaves in a power-law fashion according to the Luttinger theory with interaction-dependent exponents [30]. It was shown that the universal low-energy power-law is $\rho_\sigma(\omega) \propto |\omega|^{g_\alpha}$for $\omega \to 0$. Fig. 4 shows that in the limit of strong interaction, Zeeman splitting behavior of the dip will disappears and the DOS

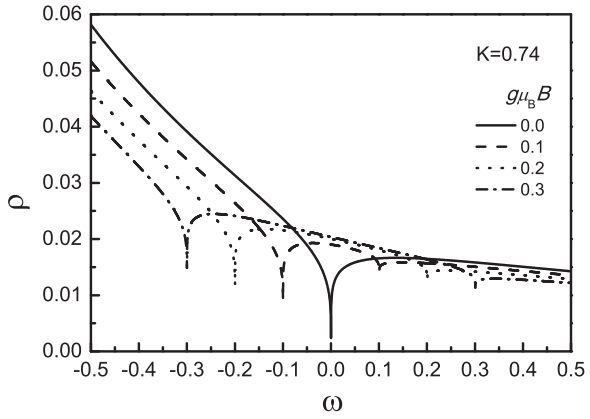

Fig. 3. The DOS as a function of energy ω for different magnetic fields and for moderately strong intra-lead interactions.

scales as a power-law function of energy.

It is well known that the key manifestation of the LL state is the existence of a power-law dependence of the tunneling DOS [22,27–29], and the power index should be just $1/g_\alpha$ when there is no magnetic field. Our work demonstrates that when a magnetic field is exerted, the power index will change, as shown in Fig. 5. When the interaction is very strong, the DOS features power-law behavior near the Fermi energy, see Fig. 5(b). The slope in Fig. 5(b) is 2.17, while when K=0.2, $1/g$=3. Thus, the power-law has been remains but the index varies when a magnetic field is present.

It is well known that the Kondo peak can be smoothed by finite temperature, which has been found using noncrossing-approximation approach [31]. The validity of the EOM approach to the Kondo problem has been proved by some authors [32]. In order to demonstrate the temperature dependence of the Kondo peak or dip, the DOS is plotted at different temperatures in Fig. 6. Indeed, the zero-bias Kondo peaks and dips are clearly visible for the low temperature and decreased with temperature increasing for weak and moderate intra-lead interactions. This behavior reflects the temperature dependence of the Kondo peak or dip in the density of states.

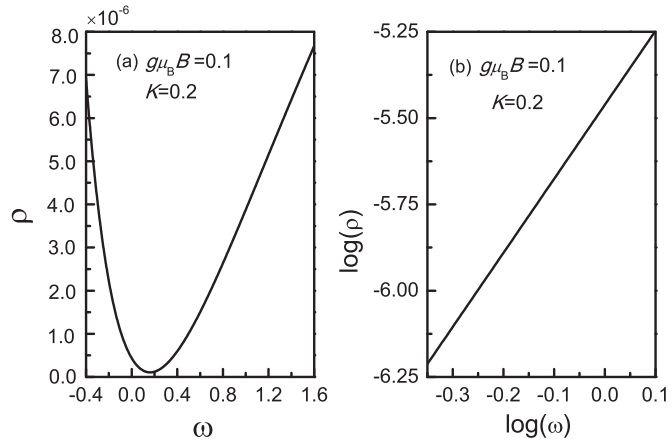

Fig. 5. (a) The DOS as functions of the level energy ω in the limit of the strong intralead interaction. (b) Double-logarithmic plot (a) in the range of $0.45 < \omega < 1.35$.The slope is 2.17.

4. Conclusion

By applying the EOM method, the joint effects of the magnetic field and electron-electron interaction in the leads on the DOS of a Kondo dot coupled to LL leads have been studied. The effects of the magnetic field on the system are summarized as follows. The Kondo peak in the DOS splits into two with the distance $2g\mu_B B$ between them, a Zeeman splitting. The two peaks belong to electrons with spin-up and spin-down, respectively. Although their distances are symmetric with respect to the original peak, the peak heights are different. With the increase of the intralead interaction, a phase transition occurs. For moderately strong interaction, the Zeeman splitting peaks develop into dips. In this case, the power-law behavior usually shown in the absent of the magnetic field does not retain. In the limit of strong interaction the Zeeman splitting behavior disappears and an approximate power-law behavior follows, but the power index deviates from$1/g$. We hope that these novel features of interacting one-dimensional electrons will stimulate other theoretical work and further experimental checks in various kinds of quantum wires, such as carbon nanotubes.

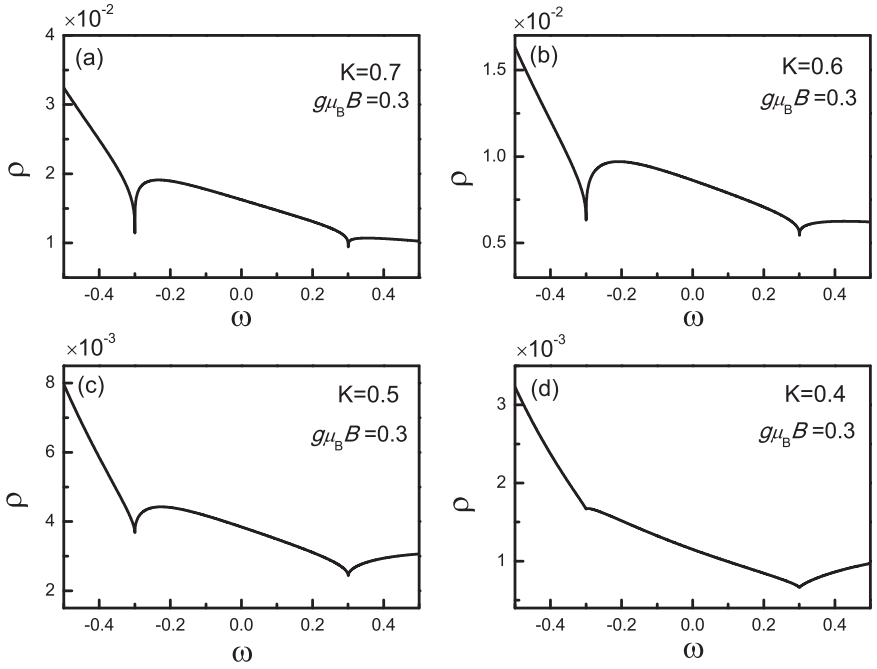

Fig. 4. The DOS as a function of energy ω for different intralead interaction under the magnetic field B=0.3.

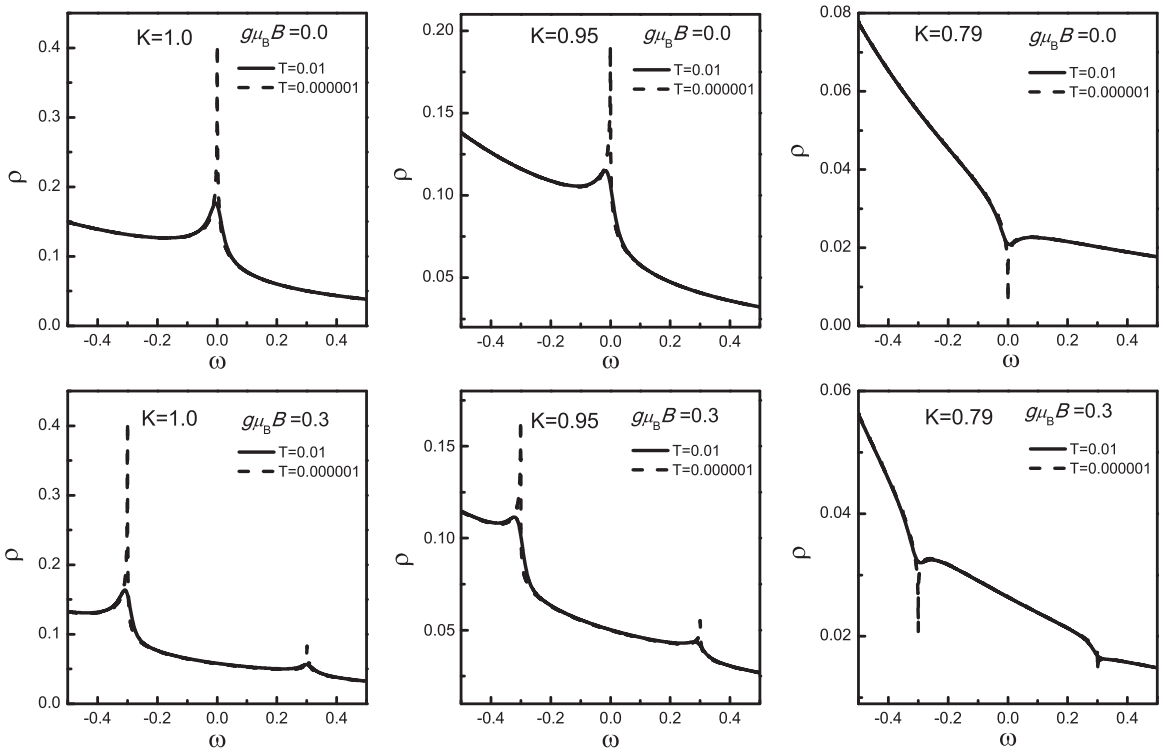

Fig. 6. The density of states at two temperatures, T=0.005 and 000001 for different intralead interaction with and without magnetic field.

Acknowledgments

This work is supported by the 973 Project of China (Grant no. 2012CB927402) and the National Natural Science Foundation of China (Grant no. 61275028).

Appendix A

Applying the equation of motion of Green's function, we have Eq. (6). The higher-order Green's function $\langle\langle\psi_{\alpha\sigma}(t); d_\sigma^\dagger(t')\rangle\rangle^r$ and $\langle\langle d_\sigma(t)n_{\bar\sigma}(t); d_\sigma^\dagger(t')\rangle\rangle^r$ appearing in that equation need to be calculated carefully. Their equations of motion are Eqs. (7) and (8).

We first calculate the commutator $[\psi_{\alpha\sigma}, H_\alpha]$in Eq. (7). Let

$$\frac{\exp(-\alpha' k/2)}{\sqrt{2K_\rho k}} = w_\rho(k),\ \frac{\exp(-\alpha' k/2)}{\sqrt{2K_\sigma k}} = w_\sigma(k) \text{ and } \int_0^\infty dk w_\rho(k)(a_{k\alpha} - a_{k\alpha}^\dagger) = \zeta_\rho,$$
$$\int_0^\infty dk w_\sigma(k)\sigma(c_{k\alpha} - c_{k\alpha}^\dagger) = \zeta_\sigma. \tag{A.1}$$

$$\psi_{\alpha\sigma} = \sqrt{\frac{2}{\pi\alpha'}}\exp(\zeta_\rho + \zeta_\sigma).$$

Here, $\zeta_\rho$and ζ_σ are commutable. Then

$$[\psi_{\alpha\sigma}, H_\alpha] = \hbar v_c\sqrt{\frac{2}{\pi\alpha'}}\sum_{n=0}^\infty\frac{1}{n!}[\zeta_\rho^n, \int_0^\infty k' a_{k'\alpha}^\dagger a_{k'\alpha}dk']e^{\zeta_\sigma} + e^{\zeta_\rho}\hbar v_s\sqrt{\frac{2}{\pi\alpha'}}\sum_{n=0}^\infty\frac{1}{n!}[\zeta_\sigma^n, \int_0^\infty k' c_{k'\alpha}^\dagger c_{k'\alpha}dk']. \tag{A.2}$$

In the first term, the lowest nonzero term is that

$$[\zeta_\rho, \int_0^\infty k' a_{k'\alpha}^\dagger a_{k'\alpha}dk'] = \int_0^\infty dk w_\rho(k)k(a_{k\alpha} + a_{k\alpha}^\dagger) \equiv \varphi_{\rho\ \alpha} \tag{A.3}$$

Then, we have

$$[\zeta_\rho^n, \int_0^\infty k' a_{k'\alpha}^\dagger a_{k'\alpha}dk'] = \sum_{i=0}^{n-1}\zeta_\rho^i\varphi_\alpha\zeta_\rho^{n-1-i} \tag{A.4}$$

Now, let us calculate that

$$[\varphi_{\rho\alpha}, \zeta_\rho] = -\frac{1}{K_\rho}\int_0^\infty dk\exp(-\alpha' k) = -\frac{1}{K_\rho\alpha'} \equiv C_\rho \tag{A.5}$$

Thisis a constant, which makes the following calculation simpler. We rewrite this commutator as$\varphi_{\rho\alpha}\zeta_\rho = \zeta_\rho\varphi_{\rho\alpha} + C_\rho$. It is easily verified that

$$\varphi_{\rho\alpha}\zeta_\rho^{n-1} = \zeta_\rho^{n-1}\varphi_{\rho\alpha} + (n-1)\zeta_\rho^{n-2}C_\rho. \tag{A.6}$$

Using (A.6) repeatedly, we obtain the results of Eq. (A.4) as follows.

$$[\zeta_\rho^n, \int_0^\infty k' a_{k'\alpha}^\dagger a_{k'\alpha} dk'] = n\zeta_\rho^{n-1}\varphi_{\rho\alpha} + \frac{n(n-1)}{2}\zeta_\rho^{n-2}C_\rho. \tag{A.7}$$

Therefore,

$$\begin{aligned}
&\hbar v_c\sqrt{\tfrac{2}{\pi\alpha'}}\textstyle\sum_{n=0}^\infty \frac{1}{n!}[\zeta_\rho^n, \int_0^\infty k' a_{k'\alpha}^\dagger a_{k'\alpha} dk']e^{\zeta_\sigma} \\
&= \hbar v_c\sqrt{\tfrac{2}{\pi\alpha'}}\textstyle\sum_{n=0}^\infty \frac{e^{\zeta_\sigma}}{n!}(n\zeta_\rho^{n-1}\varphi_{\rho\alpha} + \frac{n(n-1)}{2}\zeta_\rho^{n-2}C_\rho) \\
&= \hbar v_c\sqrt{\tfrac{2}{\pi\alpha'}}e^{\zeta_\sigma}(\varphi_{\rho\alpha} + \tfrac{C_\rho}{2})e^{\zeta_\rho} = \hbar v_c(\varphi_{\rho\alpha} + \tfrac{C_\rho}{2})\psi_{\alpha\sigma}
\end{aligned}$$

The second term in Eq. (A.2) is treated similarly, and we arrive at

$$[\psi_{\alpha\sigma}, H_\alpha] = [\hbar v_c(\varphi_{\rho\alpha} + \frac{C_\rho}{2}) + \hbar v_s(\varphi_{\sigma\alpha} + \frac{C_\sigma}{2})]\psi_{\alpha\sigma} \tag{A.8}$$

Now, we let

$$\varepsilon_{\rho/\sigma\alpha} = \hbar v_{c/s}(\langle\varphi_{\rho/\sigma\alpha}\rangle - \frac{1}{2K_{\rho/\sigma}\alpha'}), \quad \varepsilon_\alpha = \varepsilon_{\rho\alpha} + \varepsilon_{\sigma\alpha}.$$

At this stage, we make the following approximation:

$$[\psi_{\alpha\sigma}, H_\alpha] \approx \hbar v_c[(\langle\varphi_\alpha\rangle - \frac{1}{2K_\rho\alpha'}) + \hbar v_s(\langle\varphi_{\sigma\alpha}\rangle - \frac{1}{K_\sigma\alpha'})]\psi_{\alpha\sigma} \equiv \varepsilon_\alpha\psi_{\alpha\sigma}. \tag{A.9}$$

We give two reasons for this approximation. The first one is that as K=1, the derivation naturally degrades to the case of Fermi liquid conductors [8]. The second one is that the operator $a_{k\alpha} + a_{k\alpha}^\dagger$ in $\varphi_\alpha \equiv \int_0^\infty dkw(k)k(a_{k\alpha} + a_{k\alpha}^\dagger)$ is of the meaning of position operator. The integral covers all the states with the momentum as the weight. The replacement of φ_α by $\langle\varphi_\alpha\rangle$ is to replace the instant value of the averaged one, which is reasonable.

Under this approximation, Eq. (7) is rewritten as

$$(i\frac{\partial}{\partial t} - \varepsilon_\alpha) << \psi_{\alpha\sigma}(t); d_\sigma^+(t') >>^r = t_\alpha^* G_{d\sigma}^r(t, t'). \tag{A.10}$$

The case of Eq. (8) should be more careful. If simple Hartree-Fock decoupling is applied in Eq. (7), the Kondo peak will not appear in the DOS of the QD. Therefore, the equations of motion of higher-order Green's functions are inevitable. They are as follows.

$$\begin{aligned}
&(i\tfrac{\partial}{\partial t} - \varepsilon_\alpha) << \psi_{\alpha\sigma}(t)n_{\bar\sigma}(t); d_\sigma^\dagger(t') >>^r = t_\alpha^* << d_\sigma(t)n_{\bar\sigma}(t); d_\sigma^\dagger(>') >>^r + \\
&\textstyle\sum_\beta (t_\beta << \psi_{\beta\sigma}(t)d_{\bar\sigma}^\dagger(t)\psi_{\alpha\bar\sigma}(t); d_\sigma^\dagger(t') >>^r - t_\beta^* << \psi_{\beta\sigma}(t)\psi_{\alpha\bar\sigma}^\dagger(t)d_{\bar\sigma}(t); d_\sigma^\dagger(t') >>^r),
\end{aligned} \tag{A.11}$$

$$\begin{aligned}
&(i\tfrac{\partial}{\partial t} + \varepsilon_\alpha - \varepsilon_\sigma - \varepsilon_{\bar\sigma} - U) << \psi_{\alpha\sigma}^\dagger(t)d_\sigma(t)d_{\bar\sigma}(t); d_\sigma^\dagger(t') >>^r = - < \psi_{\alpha\bar\sigma}^\dagger(t)d_{\bar\sigma}(t) > + t_\alpha << d_\sigma(t)n_{\bar\sigma}(t); d_\sigma^\dagger(t') >>^r + \\
&\textstyle\sum_\beta t_\beta(<< \psi_{\beta\bar\sigma}^\dagger(t)\psi_{\alpha\sigma}(t)d_{\bar\sigma}(t); d_\sigma^\dagger(t') >>^r + << \psi_{\beta\bar\sigma}^\dagger(t)d_\sigma(t)\psi_{\alpha\bar\sigma}(t); d_\sigma^\dagger(t') >>^r),
\end{aligned} \tag{A.12}$$

$$\begin{aligned}
&(i\tfrac{\partial}{\partial t} - \varepsilon_\alpha - \varepsilon_\sigma + \varepsilon_{\bar\sigma}) << \psi_{\alpha\bar\sigma}(t)d_{\bar\sigma}^\dagger(t)d_\sigma(t); d_\sigma^\dagger(t') >>^r = - << d_{\bar\sigma}^\dagger(t)\psi_{\alpha\sigma}(t) > + t_\alpha^*[G_\sigma^r(t, t') - << d_\sigma(t)n_{\bar\sigma}(t); d_\sigma^\dagger(t') >>^r] + \\
&\textstyle\sum_\beta (t_\beta << \psi_{\beta\bar\sigma}(t)d_{\bar\sigma}^\dagger(t)\psi_{\alpha\sigma}(t); d_\sigma^\dagger(t') >>^r - t_\alpha^* << \psi_{\beta\bar\sigma}(t)\psi_{\alpha\bar\sigma}^\dagger(t)d_\sigma(t); d_\sigma^\dagger(t') >>^r).
\end{aligned} \tag{A.13}$$

In these equations, the approximation Eq. (A.9) has been employed. In order to fully decouple these equations, the method of Refs. is used [33,34]. A projection operator $\hat P$ is defined as [35]

$$\hat P(\hat O) = d_\sigma\frac{<\{\hat O, d_\sigma^\dagger\}>}{<\{d_\sigma, d_\sigma^\dagger\}>}, \tag{A.14}$$

Where$\hat O$ is an arbitrary operator, and $\{\hat O, d_\sigma^\dagger\}$ denotes its anti-commutator with $d_\sigma^\dagger$. This projection operator leads to the following approximations.

$$<< \psi_{\beta\sigma}(t)d_{\bar\sigma}^\dagger(t)\psi_{\alpha\bar\sigma}(t); d_\sigma^\dagger(t') >>^r \approx << P(\psi_{\beta\sigma}(t)d_{\bar\sigma}^\dagger(t)\psi_{\alpha\bar\sigma}(t)); d_\sigma^\dagger(t') >>^r = 0, \tag{A.15}$$

Similarly,$\langle\langle\psi_{\beta\sigma}(t)\psi_{\alpha\bar\sigma}^\dagger(t)d_{\bar\sigma}(t); d_\sigma^\dagger(t')\rangle\rangle^r$, $\langle\langle\psi_{\beta\bar\sigma}^\dagger(t)\psi_{\alpha\sigma}(t)d_{\bar\sigma}(t); d_\sigma^\dagger(t')\rangle\rangle^r$ and$\langle\langle\psi_{\beta\bar\sigma}(t)d_{\bar\sigma}^\dagger(t)\psi_{\alpha\sigma}(t); d_\sigma^\dagger(t')\rangle\rangle^r$ are also approximately zero. Two nonzero decouplins are

$$<< \psi_{\beta\bar\sigma}^\dagger(t)d_\sigma(t)\psi_{\alpha\bar\sigma}(t); d_\sigma^\dagger(t') >>^r \approx << P(\psi_{\beta\bar\sigma}^\dagger(t)d_\sigma(t)\psi_{\alpha\bar\sigma}(t)); d_\sigma^\dagger(t') >>^r = -\delta_{\alpha\beta} < \psi_{\alpha\bar\sigma}^\dagger(t)\psi_{\alpha\bar\sigma}(t) > G_{d\sigma}^r(t, t'), \tag{A.16}$$

and

$$<< \psi_{\beta\bar\sigma}(t)\psi_{\alpha\bar\sigma}^\dagger(t)d_\sigma(t); d_\sigma^\dagger(t') >>^r \approx << P(\psi_{\beta\bar\sigma}(t)\psi_{\alpha\bar\sigma}^\dagger(t)d_\sigma(t)); d_\sigma^\dagger(t') >>^r = \delta_{\alpha\beta}(1 - < \psi_{\alpha\bar\sigma}^\dagger(t)\psi_{\alpha\bar\sigma}(t) >)G_{d\sigma}^r(t, t'). \tag{A.17}$$

Besides, when tunneling t_α is small, the correlations $<\psi_{\alpha\bar\sigma}^\dagger(t)d_{\bar\sigma}(t)>$ in (A.12) and $<d_{\bar\sigma}^\dagger(t)\psi_{\alpha\bar\sigma}(t)>$ in (A.13) and are approximately zero [36].

Under these approximations, Eqs. (A.11)–(A.13) are simplified as follows.

$$(i\frac{\partial}{\partial t} - \varepsilon_\alpha) << \psi_{\alpha\sigma}(t)n_{\bar\sigma}(t); d_\sigma^\dagger(t') >>^r = t_\alpha^* << d_\sigma(t)n_{\bar\sigma}(t); d_\sigma^+(t') >>^r, \tag{A.18}$$

$$(i\frac{\partial}{\partial t} + \varepsilon_\alpha - \varepsilon_\sigma - \varepsilon_{\bar{\sigma}} - U) << \psi^\dagger_{\alpha\sigma}(t)d_\sigma(t)d_{\bar{\sigma}}(t); d^\dagger_\sigma(t') >>^r = t^*_\alpha << d_\sigma(t)n_{\bar{\sigma}}(t); d^+_\sigma(t') >>^r - t_\alpha < \psi^+_{\alpha\bar{\sigma}}(t)\psi_{\alpha\bar{\sigma}}(t) > G^r_{d\sigma}(t, t'), \tag{A19}$$

$$(i\frac{\partial}{\partial t} - \varepsilon_\alpha - \varepsilon_\sigma + \varepsilon_{\bar{\sigma}}) << \psi_{\alpha\bar{\sigma}}(t)d^\dagger_{\bar{\sigma}}(t)d_\sigma(t); d^\dagger_\sigma(t') >>^r = t^*_\alpha(G^r_{d\sigma}(t, t') - << d_\sigma(t)n_{\bar{\sigma}}(t); d^+_\sigma >>^r) - t^*_\alpha(1 - < \psi^+_{\alpha\bar{\sigma}}(t)\psi_{\alpha\bar{\sigma}}(t) >)G^r_{d\sigma}(t, t'). \tag{A.20}$$

References

[1] A.C. Hewson, The Kondo Problem to Heavy Fermions, Cambridge University Press, Cambridge, UK, 1993.
[2] (a) A.O. Gogolin, A.A. Nersesyan, A.M. Tsvelik, Bosonization and Strongly Correlated Systems, Cambridge University Press, Cambridge, 1998;
(b) T. Giamarchi, Quantum Physics in One Dimension, Oxford University Press, Oxford, 2003.
[3] D. Goldhaber-Gordon, H. Shtrikman, D. Mahalu, D. Abusch-Magder, U. Meirav, M.A. Kastner, Nature 391 (1998) 156.
[4] S.M. Cronenwett, T.H. Oosterkamp, L.P. Kouwenhoven, Science 281 (1998) 540.
[5] J. Schmid, et al., Physica 256B–258B (1998) 182.
[6] A. Kogan, S. Amasha, D. Goldhaber-Gordon, G. Granger, M.A. Kastner, H. Shtrikman, Phys. Rev. Lett. 93 (2004) 166602.
[7] D.M. Zumb¨uhl, C.M. Marcus, M.P. Hanson, A.C. Gossard, Phys. Rev. Lett. 93 (2004) 256801.
[8] S. Amasha, I.J. Gelfand, M.A. Kastner, A. Kogan, Phys. Rev. B 72 (2005) 045308.
[9] T.-M. Liu, B. Hemingway, A. Kogan, S. Herbert, M. Melloch, Phys. Rev. Lett. 103 (2009) 026803.
[10] G.D. Scott, D. Natelson, S. Kirchner, E. Mu˜noz, (R)Phys. Rev. B 87 (2013) 241104.
[11] A.A. Aligia, Phys. Rev. B 74 (2006) 155125.
[12] A. Rosch, J. Paaske, J. Kroha, P. W¨olfle, Phys. Rev. Lett. 90 (2003) 076804.
[13] A. Rosch, T. Costi, J. Paaske, P. W¨olfle, Phys. Rev. B 68 (2003) 014430.
[14] A. Rosch, J. Paaske, J. Kroha, P. W¨olfle, J. Phys. Soc. Jpn. 74 (2005) 118.
[15] A.C. Hewson, J. Bauer, A. Oguri, J. Phys.: Condens. Matter 17 (2005) 5413.
[16] P. Roura-Bas, Phys. Rev. B 81 (2010) 155327.
[17] Y. Meir, N.S. Wingreen, P.A. Lee, Phys. Rev. Lett. 70 (1993) 2601.
[18] R. L´opez, D. S´anchez, Phys. Rev. Lett. 90 (2003) 116602.
[19] Eugene H. Kim, arXiv:cond-mat/0106575v1, 2001.
[20] M. Fabrizio, A.O. Gogolin, Phys. Rev. B 51 (1995) 17827.
[21] A. Furusaki, Phys. Rev. B 57 (1998) 7141.
[22] K.-H. Yang, X. -He, H.-Y. Wang, K.-D. Liu, B.-Y. Liu, Eur. Phys. J. B 87 (2014) 172.
[23] T.K. Ng, Phys. Rev. Lett. 76 (1996) 487.
[24] K.-H. Yang, Y. Chen, H.-Y. Wang, B.-Y. Liu, Phys. Lett. A 377 (2013) 687.
[25] R. Świrkowicz, M. Wilczyński, J. Barnaś, J. Phys.: Condens. Matter 18 (2006) 2291.
[26] R. Świrkowicz, M. Wilczyński, M. Wawrzyniak, J. Barnaś, Phys. Rev. B 73 (2006) 193312.
[27] R. Egger, A. Gogolin, Effective low-energy theory for correlated carbon nanotubes, Phys. Rev. Lett. 79 (1997) 5082.
[28] C. Kane, L. Balents, M.P.A. Fisher, Coulomb interactions and mesoscopic effects in carbon nanotubes, Phys. Rev. Lett. 79 (1997) 5086.
[29] Z. Yao, H.W. Ch. Postma, L. Balents, C. Dekker, Nat. 402 (1999) 273.
[30] J.M. Luttinger, J. Math. Phys. 4 (1963) 1154.
[31] N.S. Wingreen, Y. Meir, Phys. Rev. B 49 (1994) 11040.
[32] Y. Qi, J.-X. Zhu, C.S. Ting, Phys. Rev. B 79 (2009) 205110.
[33] A.E. Ruckenstein, S. S.-Rink, Int. J. Mod. Phys. B 3 (1989) 1809.
[34] P. Fulde, Electron Correlations in molecules and solids, Spring-Verlag, Berlin, 1993.
[35] K. Kang, B.I. Min, Phys. Rev. B 52 (1995) 10689.
[36] Z.M. Hu, K.-H. Yang, G.-S. Tian, Commun. Theor. Phys. 44 (2005) 563.